Wedge-Shaped Potential and Airy-Function Electron Localization in Oxide Superlattices

Z. S. Popovic* and S. Satpathy
Department of Physics, University of Missouri, Columbia, Missouri 65211, USA
(Received 2 September 2004; published 4 May 2005)

Oxide superlattices and microstructures hold the promise for creating a new class of devices with unprecedented functionalities. Density-functional studies of the recently fabricated, lattice-matched perovskite titanates $(SrTiO_3)_n/(LaTiO_3)_m$ reveal a classic wedge-shaped potential well for the monolayer ($m = 1$) structure, originating from the Coulomb potential of a two-dimensional charged La sheet. The potential in turn confines the electrons in the Airy-function-localized states. Magnetism is suppressed for the monolayer structure, while in structures with a thicker $LaTiO_3$ part, bulk antiferromagnetism is recovered, with a narrow transition region separating the magnetic $LaTiO_3$ and the nonmagnetic $SrTiO_3$.

DOI: 10.1103/PhysRevLett.94.176805 PACS numbers: 73.20.−r, 73.21.−b

While the growth of the atomically abrupt, lattice-matched interfaces between semiconductors has long been perfected and such structures are now widely used in electronic devices, the growth of such high-quality oxide structures has not been possible for a long time. In a recent work, Ohtomo *et al.* [1] reported the growth of atomically precise, lattice-matched superlattices made up of alternating layers of $LaTiO_3$ and $SrTiO_3$. What is striking is that the quality of the interfaces easily matched the quality of similar semiconductor structures. This has raised the hope of being able to grow quality structures using other oxides [2] as well, opening them up for new physics and potentially novel device concepts. An understanding of the interface electron states played a key role in the development of semiconductor electronics and revealed many novel features not found in the bulk constituents, e.g., the formation of the two-dimensional electron gas and the subsequent discovery of the quantum Hall effect. Analogously, the understanding of the electronic properties of the oxide interfaces will potentially lead to new physics, with the strong correlation effects providing a new twist, as compared to their semiconductor counterparts.

In this Letter, we study the interface electronic structure of the recently fabricated perovskite titanate superlattices using calculations based on the first-principles density-functional theory (DFT). An interesting finding is the formation of a wedge-shaped potential well at the interface caused by a positive La sheet-charge density. The potential in turn binds the electron at the interface, with an Airy-function-derived, localized wave function, the signature of which has been observed [1] in the experiments in the form of an exponential-like spread of the Ti^{3+} fraction near the interface. To our knowledge, this is the first time that a wedge-shaped potential has been found in any system, which opens up the possibility for studying the physics of a new two-dimensional Airy gas [3].

The bulk electronic structures of both $SrTiO_3$ and $LaTiO_3$ have been well studied. Both materials form in the perovskite crystal structure, with a three-dimensional network of corner-sharing TiO_6 octahedra [4,5]. While $SrTiO_3$ is a band insulator with an empty Ti (d^0) band, $LaTiO_3$, in contrast, is a Mott insulator with Ti (d^1) occupancy. In a simple picture, the latter can be thought of within the context of the half-filled Hubbard model, which predicts an antiferromagnetic insulator as observed. In addition, the insulating state of $LaTiO_3$ is very quickly destroyed with the introduction of a small number of holes via the addition of extra oxygen [6] or via Sr substitution (with as little as $x \approx 0.05$ for $La_{1-x}Sr_xTiO_3$) [7]. This is reminiscent of the Nagaoka state where a single hole destroys both the antiferromagnetism and the insulating behavior in the half-filled Hubbard model [8].

In contrast to this, the behavior of the electrons in superlattices such as $(SrTiO_3)_n/(LaTiO_3)_m$ is expected to be fundamentally different from that in the random alloy with the same composition. As opposed to some effective average potential due to the La ions seen by the conduction electrons [the stripped-off La (d^1) electrons] in the alloy, the potential in the superlattice is due to a coherent superposition of the Coulomb potentials of the La ions organized on lattice planes. This leads to a potential well near the La layers, in which the conduction electrons in turn become confined, leading to a metallic behavior within a Hartree-Fock theory [9].

To study the electronic structure of the $(SrTiO_3)_n/(LaTiO_3)_m$ superlattices, we have performed calculations within the local-spin-density approximation (LSDA) to the density-functional theory as well as the Coulomb corrected "LSDA + U" (LSDA + Hubbard U) method [10]. Since the LSDA + U method is necessary to describe the correlation physics for bulk $LaTiO_3$, albeit in an approximate way [11,12], we have used this method here. However, for the single-La-layer $(SrTiO_3)_n/(LaTiO_3)_1$ structure, which we found to be nonmagnetic, the Coulomb correction did not make an essential difference, and we have therefore reported the results from the LSDA calculations. The linear muffin-tin orbitals method [13] was used throughout to solve the Kohn-Sham equations. For superlattices with a thick $LaTiO_3$ part, we have used the full octahedral distortions of bulk $LaTiO_3$,

 © 2005 The American Physical Society

while for superlattices with a single $LaTiO_3$ layer, we have used undistorted octahedral structure of the embedding $SrTiO_3$.

Since a key point of these superlattices turns out to be the presence of the interfacial potential well, we first present the result for it. The variation of the potential seen by the electron at the interface may be calculated from the variation of some reference energy in the DFT calculation. A convenient reference energy that we have successfully used for the semiconductor interfaces is the cell-averaged point-charge Coulomb potential V [14]. It may be calculated by first averaging the potential parallel to the plane near the interface (planar-averaged potential) and then by averaging over a period normal to the plane. We can, alternatively, calculate V by first averaging the potential over the volume of the ith Wigner-Seitz atomic sphere:

$$V_i = \frac{3q_i}{2s_i} + \sum_j{}' \frac{q_j}{|r_i - r_j|}, \tag{1}$$

and then by averaging over all spheres with a weight factor proportional to their volumes [15]: $V = \sum_i \Omega_i V_i / \sum_i \Omega_i$, where $\Omega_i = 4\pi s_i^3/3$ is the sphere volume, s_i is the sphere radius, r_i is the sphere position, and q_i is the total charge, nuclear plus electronic. In Eq. (1), the first term is the sphere average of the potential of the point charge located at the center of the muffin-tin sphere and the second term is the Madelung potential due to all other spheres in the solid.

The cell-averaged potential $V(z)$ as a function of the distance z from the interface is shown in Fig. 1(b) for the case of the single-$LaTiO_3$-layer superlattice. The potential has a remarkable, textbooklike wedge shape, $V = -eE|z|$, which is the potential for the constant electric field near a uniform sheet of charge, leading to a novel wedge-shaped quantum well. If we spread out the La (+1) charges uniformly over the single La layer at the interface, then Gauss's law in elementary electrostatics tells us that the electric field is given by the expression $E = \sigma/2\varepsilon$, where the sheet charge density $\sigma = 1|e|/S$, S being the interface area per La atom. If we compare the computed electric field from the DFT with the field of the uniform sheet charge density, we find that the latter is screened due to the embedding $SrTiO_3$ with a large relative dielectric constant of $\varepsilon_r \approx 23$. This is not surprising, since it is well known that $SrTiO_3$ is close to being ferroelectric with an unusually large long-wavelength dielectric response of $\varepsilon \approx 30 \times 10^3$ at low temperatures [16,17]. However, the screening of the sheet charge involves the short-range dielectric response, with a smaller expected ε, consistent with the calculated electric field.

The stripped-off La (d^1) electrons, which produce the positive La sheet charge in the first place, become bound in turn in the wedge-shaped potential well. The eigenstates of the electrons are obtained from the Schrödinger equation,

$$\frac{-\hbar^2}{2m}\frac{d^2\Psi}{dz^2} + V(z)\Psi = \bar{\varepsilon}\Psi, \tag{2}$$

where $V(z) = F|z|$ is the potential of the sheet charge and $F = -eE$ is a positive constant. Defining the scaled length $l = (\hbar^2/2mF)^{1/3}$, energy $\lambda = \bar{\varepsilon}/(lF)$, and coordinate

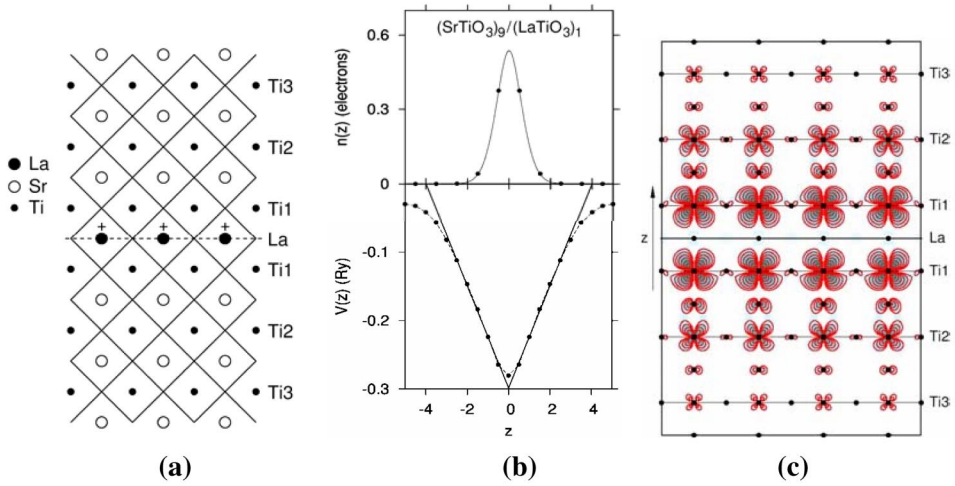

FIG. 1 (color online). The $(SrTiO_3)_n/(LaTiO_3)_1$ superlattice structure (a) with a monolayer of $LaTiO_3$ embedded in bulk $SrTiO_3$. The positively charged La sheet produces a wedge-shaped potential (b) following Gauss's law. In the bottom part of (b), the dots denote the cell-averaged electrostatic potential $V(z)$ calculated from Eq. (1) with distance z from the interface in units of the $SrTiO_3$ monolayer thickness, while the solid V-shaped line is a fit corresponding to a uniformly charged sheet. The potential confines the stripped-off La (d^1) electrons in the interface region (c). The contours show the electron charge density, integrated between the conduction bottom and the Fermi energy, indicating the electron leakage into about three Ti layers on either side of the interface. The top part of (b) shows the electron density $n(z)$, which is integrated over a perovskite layer at the position z, with the solid line being a fit using the lowest-energy Airy function. These results were calculated within the LSDA. Contour values for (c) are $\rho_n = \rho_0\ 10^{n\delta}$, where $\rho_0 = 3.4 \times\ 10^{-3}\ e/\text{Å}^3$, $\delta = 0.31$, and n labels the contours.

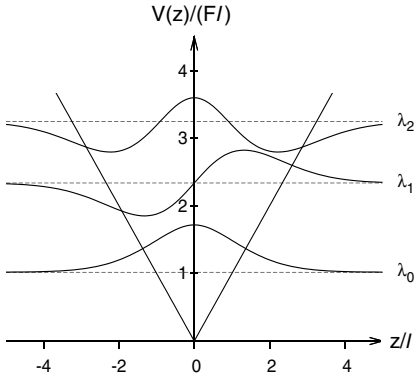

FIG. 2. Lowest eigenstates of the electron in the wedge-shaped potential well of a uniform sheet-charge density, obtained from Eq. (2), with length and energies in scaled units (see text).

$\xi = z/l - \lambda$, the Schrödinger equation takes the form $d^2\Psi/d\xi^2 - \xi\Psi = 0$, whose solutions are the well-known Airy functions $\mathrm{Ai}(\xi)$. The complete solutions are obtained by joining the Airy functions at the interface ($z = 0$) and then by matching the function or its derivative: $\mathrm{Ai}(-\lambda) = 0$ or $d\mathrm{Ai}(\xi)/d\xi|_{\xi=-\lambda} = 0$, for the odd and even parity states, respectively. The eigenvalues are given as [18] $\lambda_n \approx [3\pi(2n + 1)/8]^{2/3}$, $n = 0, 1, 2, \ldots$, an approximation that is accurate for large n, but not too bad even for the lowest n's. The Airy function decays asymptotically as $\mathrm{Ai}(z) \sim (1/2)\pi^{-1/2}z^{-1/4}\exp(-2z^{3/2}/3)$, leading to an exponential-like decay of the wave functions at large distances. The lowest three eigenstates are shown in Fig. 2.

The lowest of the Airy states is occupied in the superlattice, resulting in a rapid decay of the charge of the electron away from the $LaTiO_3$ layer, as may be seen from the densities of states (Fig. 3). The electronic charge is predominantly Ti (d) like, located mostly on the Ti1 atoms and decaying rapidly as one moves away from the sheet [see also Fig. 1(c)]. The calculated core level energies systematically track the wedge-shaped potential as well. For the general superlattice with several $LaTiO_3$ layers, the strong electric field exists only at the interfaces, leading to a quantum-well-like potential rather than the wedge-shaped potential.

The number of electrons occupying different layers may be obtained by integrating the density of states (DOS) from the conduction bottom to the Fermi energy for each perovskite layer as a function of its distance from the La sheet. The layer charges, so calculated, are shown by circles in the top part of Fig. 1(b) and they fit quite well to the shape of the lowest-energy Airy function (solid line). The length scale of the Airy function obtained from this fit is $l = 3.0$ Å, in excellent agreement with the expected value $l = (\hbar^2/2mF)^{1/3} = 2.4$ Å, using the calculated electric field and the bare electron mass. Since the ground-state Airy function spreads to about $\sim 3l$ on either side of the potential well, the electron wave function spreads to two to three layers of $SrTiO_3$ (since the layer thickness ≈ 3.91 Å). The spread is in excellent agreement with the same obtained from the experimental EELS (electron energy loss spectroscopy) profile of Ti^{3+} after deconvoluting it using the EELS profile for La. The latter serves as an effective resolution function [19], as suggested by a comparison between the EELS data and the annular-dark-field image for La [1].

The Fermi surface is shown in Fig. 4, which consists of five interpenetrating bands, the wave function characters of which are indicated in the lower right corner of the figure for the Γ point in the Brillouin zone. The orbital components of these levels are easily understood using insights from band calculations for the bulk materials [12,20,21]. The octahedral crystal field splits t_{2g} below e_g for Ti, while for La e_g is below t_{2g}. Furthermore, since the d orbital of

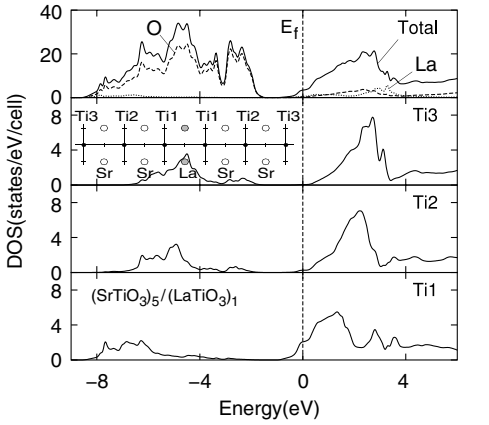

FIG. 3. Energy- and atom-resolved DOS (from LSDA), indicating the rapid decay of the Ti charge [mostly Ti (d)] as one moves away from the La sheet. In fact, note that very little Ti conduction charge is visible in the figure for Ti layers beyond Ti1.

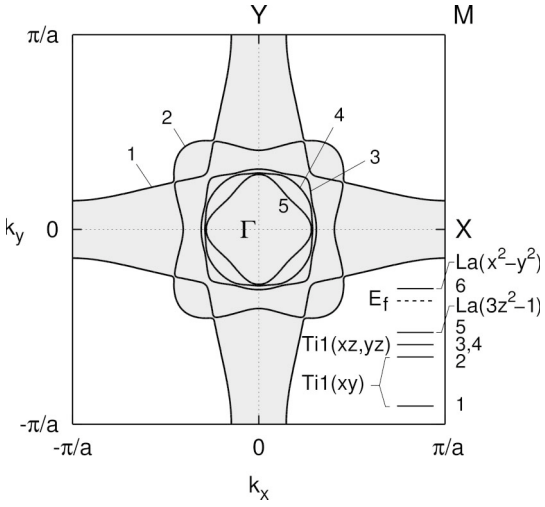

FIG. 4. The Fermi surface of $(SrTiO_3)_5/(LaTiO_3)_1$ shown in the surface Brillouin zone of the superlattice and its wave function character indicated in the lower right part of the figure (from LSDA).

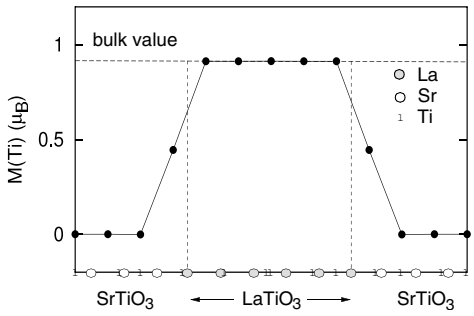

FIG. 5. Magnetic moments of the Ti atoms indicating the magnetic transition region at the interface for $(SrTiO_3)_4/(LaTiO_3)_6$, calculated using the LSDA + U method.

La has somewhat higher energy than Ti, it is clear that the Ti1 (t_{2g}) electrons should have the lowest energy on account of their placement near the bottom of the wedge-shaped potential well. Of these, the two d_{xy} states, corresponding to the two Ti1 layers on either side of the La sheet have the lowest energy. Next come the doubly degenerate Ti1 d_{yz} and d_{zx} orbitals, four in total, which are split into bonding and antibonding states, the latter occurring above the Fermi energy E_f. The next one up, the highest of the five states below E_f, is the La ($z^2 - 1$) state, again helped by its location at the bottom of the potential well. Above that is the La ($x^2 - y^2$) state and so on.

The magnetic behavior of the superlattices show some interesting features as well. For the single $LaTiO_3$ layer structures ($m = 1$), we find the paramagnetic state to be stable (both in the LSDA and the LSDA + U calculations), rather than the antiferromagnetic state of the bulk $LaTiO_3$. The paramagnetism may be rationalized by the fact that the leakage of the Ti (d^1) electronic wave function into the $SrTiO_3$ part substantially reduces the magnitude of the Coulomb U, diminishing the tendency towards magnetism. Along the same lines, we may reason that, for a sufficiently thick $LaTiO_3$ part, the inner layers would be antiferromagnetic (bulklike behavior), while the outer Ti layers would have either reduced moments or may even become paramagnetic.

To test these ideas, we have performed a LSDA + U calculation for the $(SrTiO_3)_4/(LaTiO_3)_6$ superlattice structure, which has a six-monolayer thick $LaTiO_3$ part, taking the Coulomb and exchange parameters to be $U = 5$ eV and $J = 0.64$ eV, respectively, following earlier authors [12]. The results, shown in Fig. 5, indicate the $LaTiO_3$ part to be antiferromagnetic, with the Ti moments equal to the theoretical bulk value ($\sim 0.9\mu_B$) obtained within the local density approximation. In addition, the two adjacent Ti layers at the interface with the $SrTiO_3$ region acquire a sizeable magnetic moment (about half of the bulk value) due to their proximity to the magnetic region. The magnetic moments of the rest of the Ti layers in the $SrTiO_3$ region are zero.

In conclusion, we have shown the formation of a quantum well with a textbooklike wedge-shaped potential originating from a uniformly charged interfacial La layer in the $(SrTiO_3)_n/(LaTiO_3)_1$ superlattices. The electronic structure is explained in terms of the Airy-function localization of the electrons leaking out of the $LaTiO_3$ layer, which become bound in the wedge-shaped potential well. With a $LaTiO_3$ region of several layers thick, the inner layers show bulklike antiferromagnetic behavior, while the magnetism disappears in the embedding $SrTiO_3$ layers with a narrow transition region between them.

This work was supported by the U.S. Department of Energy under Grant No. DE-FG02-00ER45818.

*Permanent address: Institute for Nuclear Sciences, "Vinca," P.O. Box 522, 11001 Belgrade, Serbia and Montenegro.

[1] A. Ohtomo, D. A. Muller, J. L. Grazul, and H. Y. Hwang, Nature (London) **419**, 378 (2002).
[2] H. Yamada, Y. Ogawa, Y. Ishii, H. Sato, M. Kawasaki, H. Akoh, and Y. Tokura, Science **305**, 646 (2004).
[3] W. Kohn and A. E. Mattsson, Phys. Rev. Lett. **81**, 3487 (1998).
[4] *Numerical Data and Functional Relations in Science and Technology—Crystal and Solid State Physics*, edited by T. Mitsui and S. Nouma, Landolt-Bornstein, New Series, Group III, Vol. 16, Pt. (a) (Springer, Berlin, 1982).
[5] M. Cwik *et al.*, Phys. Rev. B **68**, 060401 (2003).
[6] Y. Taguchi *et al.*, Phys. Rev. B **59**, 7917 (1999).
[7] Y. Tokura, Y. Taguchi, Y. Okada, Y. Fujishima, T. Arima, K. Kumagai, and Y. Iye, Phys. Rev. Lett. **70**, 2126 (1993).
[8] Y. Nagaoka, Phys. Rev. **147**, 392 (1966).
[9] S. Okamoto and A. J. Millis, Nature (London) **428**, 630 (2004).
[10] For a review, see V. I. Anisimov, F. Aryasetiawan, and A. I. Lichtenstein, J. Phys. Condens. Matter **9**, 767 (1997).
[11] I. Solovyev, N. Hamada, and K. Terakura, Phys. Rev. B **53**, 7158 (1996).
[12] E. Pavarini, S. Biermann, A. Poteryaev, A. I. Lichtenstein, A. Georges, and O. K. Andersen, Phys. Rev. Lett. **92**, 176403 (2004).
[13] O. K. Andersen and O. Jepsen, Phys. Rev. Lett. **53**, 2571 (1984).
[14] S. Satpathy, Z. S. Popovic, and W. C. Mitchel, J. Appl. Phys. **95**, 5597 (2004).
[15] W. R. L. Lambrecht, B. Segall, and O. K. Andersen, Phys. Rev. B **41**, 2813 (1990).
[16] T. Sakudo and H. Unoki, Phys. Rev. Lett. **26**, 851 (1971).
[17] K. A. Müller and H. Burkard, Phys. Rev. B **19**, 3593 (1979).
[18] M. Abramowitz and I. A. Stegun, *Handbook of Mathematical Functions* (National Bureau of Standards, Washington, DC, 1972).
[19] H. Y. Hwang (private communication).
[20] S. Kimura, J. Yamauchi, M. Tsukada, and S. Watanabe, Phys. Rev. B **51**, 11 049 (1995).
[21] I. V. Solovyev, Phys. Rev. B **69**, 134403 (2004).